In vivo determination of mechanical properties of the human ulna by means of mechanical impedance tests: Experimental results and improved mathematical model*

Gerald A. Thompson

Control Data Corporation, Sunnyvale, Cal., USA

Donald R. Young

Environmental Physiology, NASA Ames Research Centre, Moffett Field, California, USA

David Orne

Department of Mechanical Engineering, Wayne State University, Detroit, Mich. 48202, USA

Abstract—*An experimental technique and associated apparatus for measuring* in vivo *the mechanical impedance of the human ulna are described in detail. An electromagnetic shaker is used to apply a steady-state harmonic excitation to the ulna near its mid-span and measurements of the complex driving-point impedance are made. Both stiffness and resonant frequency information, useful in assessing the mechanical integrity of bone, are inferred from the impedance measurements by means of a third-generation mathematical model of the system. Results for three male and two female test subjects are reported.*

Keywords—*Human ulna, Mechanical impedance, Resonant frequency, Bone, Mathematical modelling*

Nomenclature

L = span length of beam model of the ulna, cm
a = distance from olecranon process to point of load application, cm
r = external radius of tubular beam model of ulna, cm
ξ = ratio of internal radius to external radius of tubular beam model
α = shape factor for computing moments of inertia
E = Young's modulus, N/m^2
ω_n = undamped fundamental frequency of beam (or musculature) model, Hz
ζ = damping ratio of beam (or musculature) in its first (fundamental) mode of free vibration
ρ = density of beam, g/cm^3
$I = \alpha\pi r^4(1-\xi^4)/4$ = second moment of area of beam cross-section, cm^4
$A = \pi r^2(1-\xi^2)$ = area of beam cross-section
$\mu = \rho A$ = mass per unit length of beam, g/cm
η = viscous modulus of musculature, N-s/m^2
b = effective width of musculature rod model, cm
l = effective height of musculature rod model, cm
k = elastic spring constant (depends on preload) for tissue under impedance head, N/m
c = viscous coefficient for tissue under impedance head, N-s/m

Introduction

THE DEVELOPMENT of satisfactory methods for measuring bone mechanical properties *in vivo* can provide estimates of the mechanical integrity of bones. To achieve a reliable technique of performing such measurements, the experimental procedure must be designed to obtain reproducible results, and an accurate theoretical model of the experiment must be developed which allows interpretation of the results. A systematic comparison of experimental data with theory is required to safeguard against the possibility of acquiring a volume of data which in the final analysis does not accurately reflect the properties of bones tested. Furthermore, a step-by-step comparison of experiment and theory is required to suggest improvements in the experimental method, and allows the simplest theory to be developed which includes the most important variables.

The method used to perform *in vivo* mechanical tests on appendicular bones can be either a wave-transmission test or the measurement of steady-state vibration characteristics. A study which investigated the *in vivo* measurement of wave propagation speeds was done by ANAST *et al.* (1958) where measurements were made of the transmission time for ultrasonic waves in the tibia. These results showed reduced propagation speeds in patients with fractures and osteoporotic subjects compared to normal adult males. *In vivo* measurements of steady-state vibrations excited in the ulna have been performed by JURIST (1970*a*, *b*), where a resonant frequency measurement was used as a direct index of the integrity of the ulna. A difficulty with the use of a resonant frequency as an index of the status of a bone is that, in vibrating systems, resonant frequencies in general depend on a ratio of stiffness to mass. A bone which has a reduced load-carrying capability may have both a reduced stiffness and mass and could display normal resonant frequency characteristics.

A steady-state vibration measurement technique which determines resonant frequencies as well as

* *First received 8th July and in final form 4th August 1975*

stiffness directly is the mechanical-impedance approach. CAMPBELL and JURIST (1971) have applied this technique to excised ulna and DOHERTY (1971) has performed impedance tests on tibia cadaver preparations. The results obtained by DOHERTY show that one of the difficulties with performing *in vivo* measurements is that the soft tissue layer between the driving probe and the underlying bone can contribute markedly to the impedance response.

THOMPSON (1973) devised an *in vivo* impedance measurement technique for the ulna where the dependence of the results on the properties of the soft tissue was reduced by varying the magnitude of the static preload force used to couple the vibrations to the ulna. The results reported by THOMPSON (1973) were limited to a single subject and the theoretical model used to interpret the results represented the ulna as a single degree-of-freedom oscillator and the soft tissue layer as a spring. Although the model showed good agreement with the measured response at low frequencies, at higher frequencies the simplified discrete element model did not match the data.

ORNE (1974) developed an improved model of the ulna by representing it as a uniform viscoelastic beam with the overlying soft tissue layer modelled as a 3-parameter visco-elastic solid. ORNE and MANDKE (1975) accomplished further improvements to the theoretical model by introducing the effects of a uniformly distributed tissue mass surrounding the bone and having elastic and viscous resistance.

The purpose of this paper is to provide a number of comparisons between the measured ulna impedance response of five human (three male and two female) subjects and the theoretical response predicted by an even further improved version of Orne and Mandke's theoretical model. The experimental procedure is described in detail, followed by a discussion of the improved theoretical model. The accuracy of the model in simulating experimental impedance data is quantified by means of the r.m.s. values of the difference between theoretical values and experimental data over a given frequency range.

Experiment design

A diagram of the equipment used to measure ulnar impedance is shown in Fig. 1. The electromagnetic shaker for generating the motion and forces transmitted to the subject's forearm was located on the end of a balance beam. This allowed the magnitude of the preload force used to couple the vibrations to the forearm to be adjusted by changing the position of a counterweight located at the opposite end of the balance beam. Calibration of the preload force magnitude was accomplished by attaching a weight which corresponded to the desired preload force to the driving probe and then balancing the beam.

The electromagnetic shaker employed was a Ling Model 201 unit which was modified by adding a booster spring to the moving element to prevent bottoming of the armature assembly under static preloads as high as 9·80 N (Newtons). To drive the shaker a low-distortion auto oscillator and amplifier were used. The vibration-generation system was capable of producing low-distortion harmonic signals in the frequency range from 40 Hz to 4 kHz.

A Wilcoxon Research impedance head (Model Z-11) was used to determine both the driving force and acceleration. Since the force and acceleration transducers were piezo-electric crystals, charge amplifiers (Endevco) were used as signal conditioners

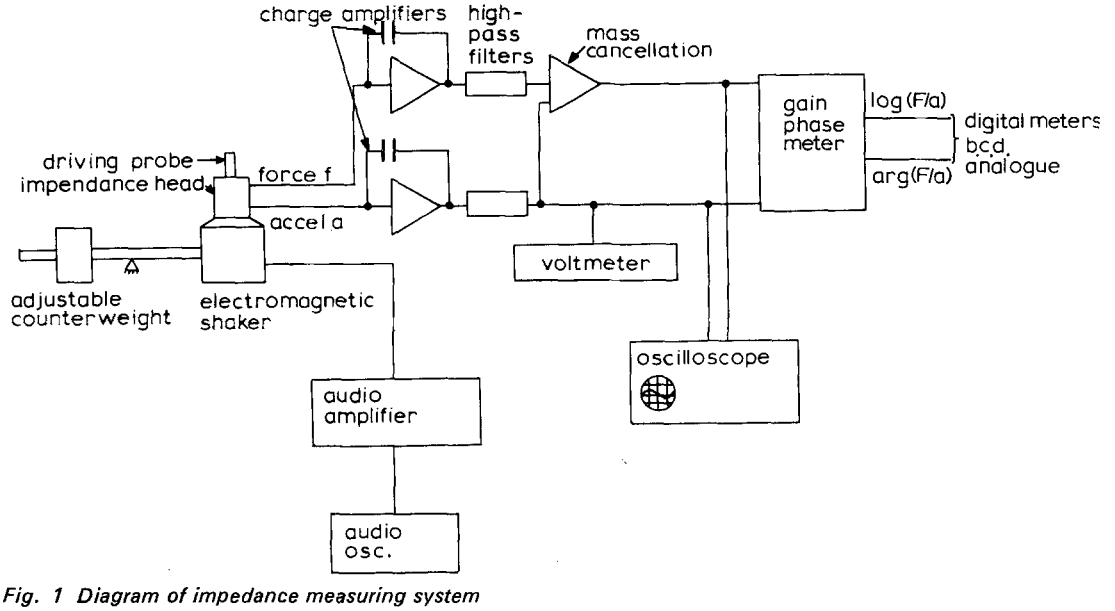

Fig. 1 Diagram of impedance measuring system

to provide voltage signals proportional to force and acceleration. As shown in Fig. 1, the charge-amplifier outputs were filtered using a pair of 4-pole active networks (Multimetrics) with matched phase and attenuation characteristics to eliminate spurious low-frequency noise. Mass cancellation was accomplished using an operational-amplifier circuit to correct the force gauge signal for the effects of mass above the force gauge, which includes that of the driving probe and the impedance head tip.

During recording of the impedance measurements for the subject's forearms, the magnitude of the acceleration of the driving probe was maintained at a constant level of 0·08 g zero-to-peak. At this acceleration level the ulnar impedances were found to be independent of amplitude, and hence the response was judged to be linear. The acceleration amplitude was monitored on an a.c. voltmeter, and both the force gauge and accelerometer signals were displayed on an oscilloscope as shown in Fig. 1.

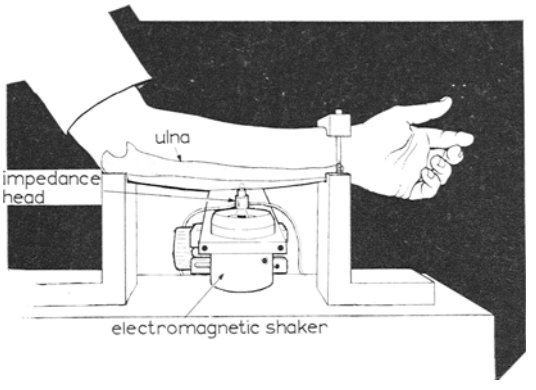

Fig. 2 Arm supports and driving system

Recording of the impedance data was done from the digital display on a gain-phase meter (Hewlett Packard Model 3573A) which presented both the ratio of force to acceleration amplitude and the associated phase angle. The measurements were recorded at discrete frequencies between 65 and 1000 Hz. Calibrations of the force gauge, accelerometer and charge-amplifier system used were performed and the accuracy of the impedance head was examined as a function of preload force at the driving probe. The sensitivities were found to be independent of preload force over the range from zero to 9·8 N.

To perform the impedance measurements the subject's arm was placed in the supports which are depicted in Fig. 2. Small plaster pads were cast to conform to bony prominences at both the wrist and elbow. The elbow pad was positioned transversely to the ulna and centred under the greater sigmoid cavity, so that, when the subject pushed downward through the humerus, the ulna was constrained from moving. Motion of the ulna at the distal end was inhibited by placing the plaster pad directly under the styloid process and applying downward pressure through the styloid end of the radius with the clamping fixture shown in Fig. 2. Using this method of positioning the forearm, the results were found to be relatively independent of the magnitude of the constraining forces at the elbow and the wrist. The location of the point at which vibrations were excited was approximately 60% of the distance from the olecranon end of the ulna to the styloid process. The transverse position of the driving probe relative to the subject's arm was determined by scanning across the forearm at a fixed frequency of 100 Hz until a position was found where the impedance was maximum. This probe position was judged to correspond to the point at which the overlying soft tissue layer was of minimum thickness.

For each subject the impedance measurements were performed in at least three separate trials to ensure that uncertainties regarding the probe location and arm position were not significantly modifying the results. After each trial, the subject's arm was removed from the constraining supports. The impedance data calculated represent an average of the three or more separate trials.

An important factor for *in vivo* mechanical impedance measurements is the choice of the effective area of the driving probe. The optimum probe would produce the greatest amount of stiffening of the tissue overlying the bone for a given preload force so that the measurements could be performed without uncomfortably high static preloads. If the skin-tissue layer responses were independent of the static preload, as in a linear system, then the impedance of a layer would be directly proportional to the probe area and a larger driving probe area would be desirable. To examine the impedance of a soft tissue layer directly, measurements were obtained on the soft tissue layer between a subject's

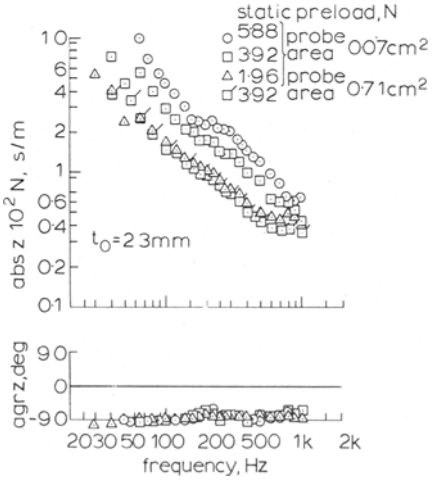

Fig. 3 Impedance of a layer of soft tissue when statically compressed

thumb and index finger. The results are shown in Fig. 3 for a range of preloads and for two driving probe areas. During these measurements the skin layer was pressed against a rigid surface. The behaviour of the soft tissue layer is predominantly spring-like as shown, and the effective stiffness increases with increasing preload force. The results indicate that for a preloading force of 3·92 N the stiffness of the soft tissue is greater for the smaller-size driving probe (7 mm² area). Hence, these data show that the behaviour of a soft tissue layer is inherently nonlinear and for performing ulnar impedance measurements the smaller-sized driving probe should be used since it achieves a higher effective stiffness for the soft tissue layer.

Further reductions in the driving probe area below 7 mm² were found to be somewhat uncomfortable for the subjects during ulnar impedance tests. Thus a driving probe area of 7 mm² was judged to provide a good trade-off between comfort and the amount of stiffening of the soft tissue layers.

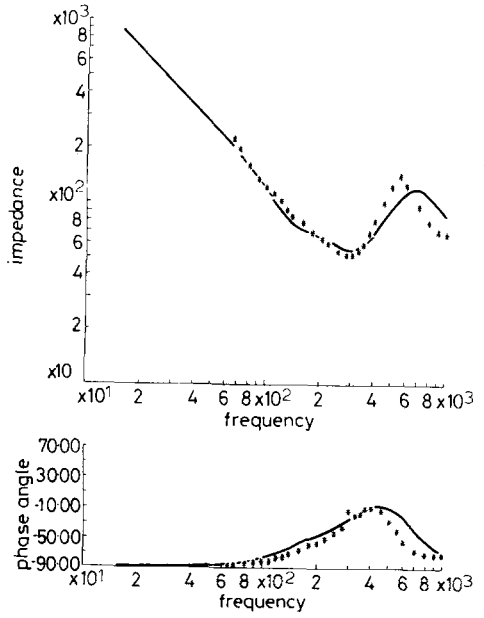

Fig. 4 Absolute impedance, |Z'| and phase angle, arg Z, versus forcing frequency, p Subject TT: 3·92 N preload.

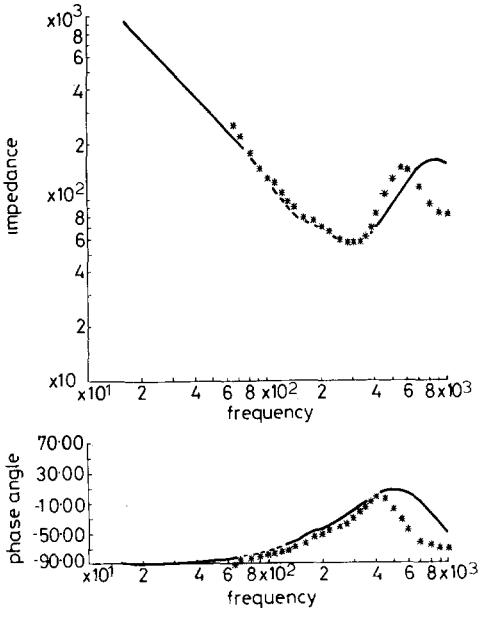

Fig. 5 Absolute impedance, |Z|, and phase angle, arg Z, versus forcing frequency, p Subject TT: 4·90 N preload.

Analysis of experimental data

ORNE (1974) and ORNE and MANDKE (1975) have developed mathematical models to simulate ulnar mechanical impedance experiments such as those described above. The first version of the model (ORNE, 1974) consisted of a simply-supported viscoelastic beam subjected to a harmonically varying force near its midspan. The soft tissue compressed between the impedance head and the ulna was modelled as a tri-parameter viscous solid whose material constants are functions of the static component (preload) of the forcing function. Some effective mass of the musculature surrounding the ulna was assumed to move with the beam (ulna) and the beam was assumed to be constructed of a Kelvin material (viscous element in parallel with elastic element).

Theoretical impedances obtained using the above model provide fairly good overall comparison with experimental data, especially in the low-frequency range below 100 Hz. However, the experimental data consistently showed a deviation from the theoretical model predictions at forcing frequencies in the neighbourhood of 120 Hz.

To improve the predictive capabilities of the viscoelastic beam model in this frequency range, it was postulated (ORNE and MANDKE, 1975) that a 'subresonance' occurs in the musculature surrounding the ulna, thus accounting for the little hump in the otherwise ~-shaped experimental impedance curves. Therefore, in the second version of the model, the musculature was depicted as an infinite series of damped, spring-mass oscillators attached to and vibrating with the beam (ulna). It was shown that the previous analysis (ORNE, 1974) of ulnar mechanical impedance would be applicable to the modified model if, in the previous analysis, the mass of the beam per unit length, μ, were replaced by the complex mass per unit length given by

$$\mu^* = \mu + \frac{m_D(k_D + iC_D p)}{k_D - m_D p^2 + iC_D p} \quad . \quad . \quad . \quad . \quad (1)$$

where m_D, k_D and C_D are the mass, spring constant and viscous constant (per unit length), respectively

of the musculature mass, and p is the forcing frequency of the applied transverse force. The natural frequency of the distributed oscillators was tuned to 110 Hz and the damping ratio set at 0·21. Considerable improvement in the correlation between model predictions and measured impedances was achieved in the intermediate frequency range of 100–300 Hz when the second model (ORNE and MANDER, 1975) was used.

Although the ulnar impedance model was considerably improved by representing the musculature surrounding the ulna as a series of spring-mass-dashpot oscillators, the oscillators have only one degree-of-freedom (relative to the ulna) and thus only one subresonance (near 110 Hz). In reality, the musculature is not 'lumped' and has its mass, elasticity and damping distributed throughout its volume and thus should have an infinite number of subresonances (relative to the ulna). Thus, a further meaningful refinement of the ulnar-impedance model can be achieved by representing the musculature as an infinite series of one-dimensional viscoelastic rods attached to and vibrating with the ulna and rigidly attached to and restrained against motion at their opposite ends by the radius. The assumption of an immovable radius is justified because the radius is much stiffer than the musculature and the load is applied to the ulna, not the radius.

Analytically, the effect of representing the musculature as one-dimensional (perpendicular to the beam axis) waveguides is simply to replace the real mass per unit length, μ, of the beam used in ORNE (1974) with the following complex mass:

$$\mu^* = \mu - bE_t^* \alpha^* \cot(\alpha^* l)/p^2 \quad . \quad . \quad . \quad (2)$$

where

$\alpha^* = p/\sqrt{(E_t^*/\rho_t)}$
b = effective thickness of the rod
l = effective length of the rod, clamped at both ends
E_t^* = complex modulus of elasticity of the rod
p = frequency of forcing function
ρ_t = density of rod (about 1 g/cm^3)
μ = (real) mass per unit length of the beam

Thus, using the results of ORNE (1974), the driving-point mechanical impedance of the ulna is given by

$$z = \left(\frac{1}{z_{tb}} + \frac{1}{z_b}\right)^{-1} \quad . \quad . \quad . \quad . \quad . \quad . \quad . \quad . \quad (3)$$

where

$$\frac{1}{z_b} = \frac{-ip}{2E^*I\lambda^{*3}}\left(\frac{\sinh\lambda^* a \sinh\lambda^* b}{\sinh\lambda^* L} - \frac{\sin\lambda^* a \sin\lambda^* b}{\sin\lambda^* L}\right) \quad (4)$$

$$\frac{1}{z_{tb}} = \frac{p^2\eta}{k_2^2 + p^2\eta^2} + i\frac{p[p^2\eta^2 + k_2(k_1+k_2)]}{k_1(k_2^2+p^2\eta^2)} \quad . \quad (5)$$

where z_b is the impedance of the beam relative to its supports and z_{tb} is the impedance of the tissue directly under the impedance head relative to the ulna. The modified complex mass enters into z_b through the parameter λ^*, which is given by

$$\lambda^{*4} = p^2\mu^*/E^*I \quad . \quad . \quad . \quad . \quad . \quad . \quad . \quad . \quad (6)$$

where E^* is the complex modulus of elasticity of the beam proper and I is its second moment of area. The length of the beam is denoted by L and the distance to the driving force from the olecranon and styloid processes are denoted by a and b, respectively. Two elastic spring constants, k_1 and k_2, and one viscous constant, η, are used to characterise the material properties of the tissue under the impedance head.

The complex modulus of the beam can be arbitrarily specified in the form $E^* = E_0(1+i\delta)$, where E_0 is the static Young's modulus of elasticity and δ is a function of forcing frequency p. In the present analysis, we have chosen $\delta = cp/E_0$, where c is a viscous coefficient having units of N s/m^2. Similarly, the complex modulus of the one-dimensional waveguides can be arbitrarily specified, but we choose the form $E_t^* = E_{0t}[1+i(p\eta/E_{0t})]$, where η is a viscous coefficient with units of N s/m^2.

Table 1. Undamped and damped frequencies and frequency-dependent damping ratios for the viscoelastic beam and viscoelastic rods

Complex modulus of elasticity	Undamped frequency $j = 1, 2, \ldots$	Frequency-dependent damping ratio $j = 1, 2, \ldots$	Damped frequency $j = 1, 2, \ldots$
(Beam)			
$E^* = E_0\left(1 + \frac{icp}{E_0}\right)$	$\omega_j = j^2\frac{\pi^2}{L^2}\sqrt{\frac{E_0 I}{\mu}}$	$\zeta_j = \frac{c}{2E_0}\omega_j$	$\omega_{d_j} = \omega_j\sqrt{(1-\zeta_j^2)}$
(Rod)			
$E_t^* = E_{0t}\left(1 + \frac{i\eta p}{E_{0t}}\right)$	$\omega_j = j\frac{\pi}{L}\sqrt{\frac{E_{0t}}{\rho_t}}$	$\zeta_j = \frac{\eta}{2E_{0t}}\omega_j$	$\omega_{dj} = \omega_j\sqrt{(1-\zeta_j^2)}$

Using the above relations for the complex moduli of the beam and one-dimensional waveguides, and after some analysis, it can be shown that damped normal modes of free vibration exist for both the beam and the one-dimensional waveguides. Their undamped and damped frequencies and damping ratios are given in Table 1.

Suppose that material parameters for the rods were specified such that the first *undamped* frequency occurred at $\omega_1 = 110$ Hz, with a damping

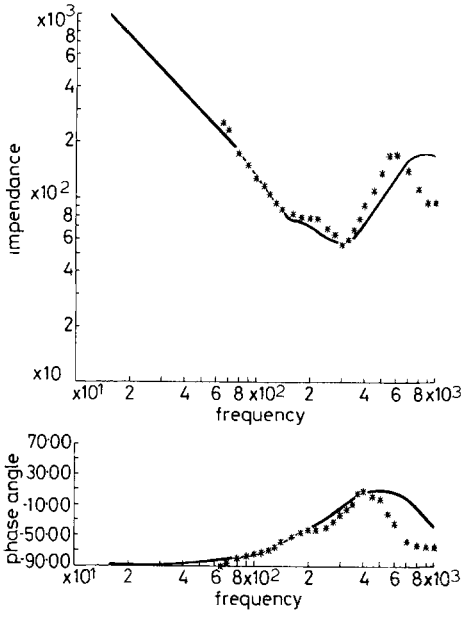

Fig. 6 Absolute impedance, $|Z|$, and phase angle arg Z, versus forcing frequency, p
Subject TT: 5·88 N preload.

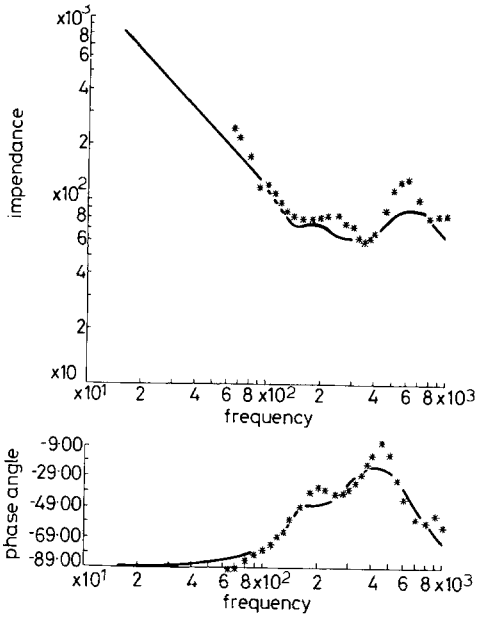

Fig. 7 Absolute impedance, $|Z|$, and phase angle, arg Z, versus forcing frequency, p
Subject CDG: 3·92 N preload.

Table 2. Values of model parameters used to simulate in vivo *impedance data for five human subjects*

		T.T., (21)♂	C.D.G., (19)♂	B.L., ( )♂	W.C., (21)♀	V.G., (22) ♀
Mineral content g/cm		0·54	0·50	0·53	0·39	0·32
Ulna width at 3 cm		1·06	1·10	1·03	0·85	0·84
Properties	L	23·4	24·2	28·35	25	21·55
of beam	a/L	0·6	0·6	0·6	0·6	0·6
(ulna)	r	0·59	0·61	0·57	0·47	0·47
	ξ	0·6	0·6	0·5	0·5	0·5
	α	2	2	2	2	2
	E	$1·52\times10^{10}$	$1·44\times10^{10}$	$2·7\times10^{10}$	$1·8\times10^{10}$	$2·4\times10^{10}$
	ω_n	400	425	400	400	400
	ζ	0·28	0·39	0·17	0·60	0·25
	ρ	1·85	1·45	1·29	0·96	1·81
	I	0·166	0·189	0·155	0·072	0·072
	A	0·700	0·748	0·765	0·520	0·520
	μ	1·295	1·085	0·990	0·501	0·942
Properties	ζ	0·4	0·3	0·3	0·2	0·3
of	ω_n	160	170	160	210	240
musculature	ρ	1·0	1·0	1·0	1·0	1·0
	η	198·4	179·9	191·2	14·5	99·2
	E	$2·5\times10^{5}$	$3·2\times10^{5}$	$3·2\times10^{5}$	$4·8\times10^{5}$	$2·5\times10^{5}$
	$b\times I$	7·4	7·9	8·4	2·5	4·9
Prop. of	k(3·92*)	$3·8\times10^{5}$	$3·0\times10^{5}$	$2·5\times10^{5}$	$2·2\times10^{5}$	$2·7\times10^{5}$
soft tissue	k(4·90)	$6·0\times10^{5}$	$4·0\times10^{5}$	$3·7\times10^{5}$	$3·7\times10^{5}$	$3·7\times10^{5}$
under impe-	k(5·80)	$6·7\times10^{5}$	$4·7\times10^{5}$	$4·0\times10^{5}$	$6·6\times10^{5}$	$4·0\times10^{5}$
dance head	c	2×10^{5}	2×10^{5}	2×10^{5}	2×10^{5}	2×10^{5}

* Preload in newtons

ratio of $\zeta_1 = 0{\cdot}20$. Then we see from Table 1 that the higher undamped frequencies of the rod are $\omega_2 = 220$ Hz, $\omega_3 = 330$ Hz etc., and the corresponding damping ratios are $\zeta_2 = 0{\cdot}40$, $\zeta_3 = 0{\cdot}60$ etc. Thus, the higher modes are more heavily damped, and according to the values assumed for the first mode, critical damping would occur at an undamped frequency of about 550 Hz.

Although the spring-mass-dashpot oscillator representation of the musculature clearly showed (analytically) how the presence of musculature can mask the overall impedance of the forearm system at frequencies near the resonant frequency of the oscillators, this influence drops off rapidly at higher frequencies. This is because the oscillators are one-degree-of-freedom systems which have the potential of simulating only one subresonance, say the one at about 110 Hz, whereas the continuous one-dimensional waveguides described above are anatomically more meaningful and have 'subresonant' frequencies over a much wider spectrum. Certainly, there is no difficulty in matching the fundamental (first) frequency and damping ratio of the one-dimensional waveguides to that of the lumped-parameter model, and letting the other frequencies and damping ratios fall where they may.

Therefore, we shall use as the latest version of the model of mechanical impedance of the ulna the one which models the musculature as essentially a viscoelastic foundation with mass. The foundation continuously supports the ulna and the foundation itself is supported by a 'rigid' radius. The complex mass of the system is given by eqn. 2 and the impedance by eqn. 3.

Results

The results have been programmed for solution on a digital computer and are used to simulate the impedance data shown in Figs. 4–9. Data were simulated for five human subjects, three male and two female, at preloads of 3·92 N, 4·90 N and 5·88 N each. The parametric values used in the mathematical model are given in Table 2 and the symbols are defined in the nomenclature list at the end of the paper. Some of the parametric values used are the result of direct measurement and others are estimated or computed from observed data.

For example, the span length L is obtained by direct measurement after the forearm is positioned in the test apparatus. Photon-absorption methods are used to measure both the width of the ulna and its bone mineral content per unit *length* at a point 30 mm from its distal end.

For subject T.T., the bone width at this point is 10·6 mm and the bone mineral content is 0·54 g/cm. We have taken the radius of the uniform beam model to be 1·11 times the radius at 30 mm, or $r = 1{\cdot}11 \times (10{\cdot}6/2) = 5{\cdot}9$ mm. Assuming the bone mineral is uniformly distributed over the volume of the bone, we estimate that the bone mineral content for the beam model is $(0{\cdot}54)(1{\cdot}11)^2 = 0{\cdot}67$ g/cm. The bone mineral content per unit *volume* is then

$$b = 0{\cdot}67/(\pi \times 0{\cdot}59^2 \times (1 - 0{\cdot}6^2)) = 0{\cdot}956 \text{ g/cm}^3$$

where it has been assumed that ξ (the internal radius divided by the external radius of the beam) is equal to 0·60.

Now, JURIST and KIANIAN (1973) suggest that, for normal human bone,

$$\left.\begin{aligned} b &= 1{\cdot}1806\rho - 1{\cdot}1945 \\ \rho &= 1{\cdot}2586 + 3{\cdot}6429 \times 10^{-12} E \end{aligned}\right\} \quad . \quad . \quad (7)$$

With $b = 0{\cdot}956$ g/cm^3 for subject T.T., the corresponding values for ρ and E are 1821·6 kg/m^3 and $1{\cdot}5456 \times 10^{10}$ N/m^2, respectively. However, ρ and E must also satisfy the relation for the undamped

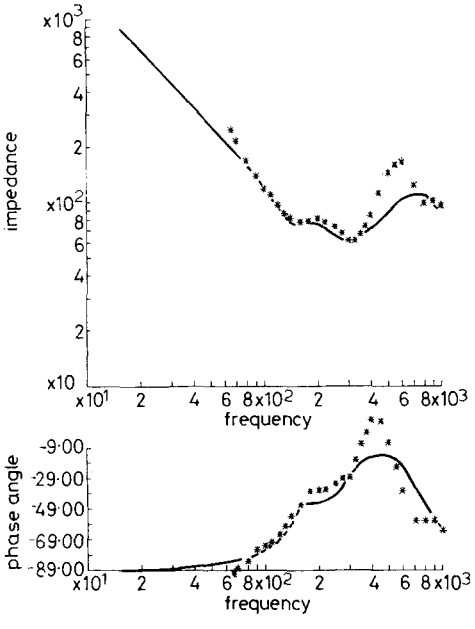

Fig. 8 Absolute impedance, $|Z|$, and phase angle, arg Z, versus forcing frequency, p
Subject CDG: 4·90 N preload.

resonant frequency of the beam given by

$$\omega_n = (\pi/2L^2)(EI/\mu) \text{ hertz} \quad . \quad . \quad . \quad . \quad . \quad (8)$$

where $\mu = \rho A$ is the mass per unit length of the beam and EI is the effective flexural stiffness of the beam.

In order not to infer unreasonable values of E from the model, it is necessary to represent the moment of inertia of the beam by

$$I = \alpha\pi r^4(1 - \xi^4)/4 \quad . \quad . \quad . \quad . \quad . \quad . \quad . \quad (9)$$

where α is adjusted to yield the proper value for EI. From parametric studies with the model, it was found that $\alpha = 2$ gave good results ($\alpha = 1$ represents

a circular tube). There is an anatomical rationale for using a value of α greater than unity: the cross-section of the ulna is tear-shaped near its mid-span and in the test configuration the ulna is forced to bend about its strong axis. The moment of inertia about the strong axis of the ulna is much greater than $I = \pi r^4(1-\xi^4)/4$, (for a circular tube), where r is one-half the ulna width. To determine a precise value for α at any cross-section requires sectioning the ulna and obtaining co-ordinates on the cross-section from which the moment of inertia can be computed. Then,

$$\alpha = I_{actual}/\{\pi r^4(1-\xi^4)/4\} \quad . \quad . \quad . \quad . \quad . \quad (10)$$

We have found in parametric studies with the mathematical model that the undamped frequency at first resonance is about 100 Hz greater than the corresponding damped frequency (which occurs at the first local minimum on the impedance/frequency curves). Thus, for subject T.T. the first local minimum occurs at about 300 Hz; so the undamped frequency occurs at about 400 Hz.

This value for the undamped resonant frequency can be matched by the model if we let $\alpha = 2$, $\rho = 1850\,kg/m^3$, $E = 1{\cdot}52 \times 10^{10}\,N/m^2$, $L = 234\,mm$ and $r = 5{\cdot}9\,mm$. A damping ratio in the beam of $\zeta = 0{\cdot}28$ is needed to match the *damped* resonant frequency point near 300 Hz. Observe that the values for ρ and E are very close to the values which satisfy eqn. 7 for a bone mineral content of $b = 956\,kg/m^3$. Of course, if such good correlation existed in clinical applications, it would be necessary to measure only the bone mineral content and bone geometry and the impedance tests would be unwarranted. Instead, the fact that the above parametric values for subject T.T. appear to satisfy both impedance data and known relationships for normal bone (our subjects are classed as normal with regard to impedance tests) simply lends credence to the interpretive capabilities of the proposed mathematical model. In cases of bone-fracture healing, bone mineral loss due to extended bed rest or weightlessness, metabolic osteoporosis etc., one cannot expect the relationships of eqn. 7 to continue to govern; and therefore the proposed impedance tests and mathematical model can provide useful estimates of the structural integrity of the ulna by providing *in vivo* measures of its stiffness, strength and resonant frequency.

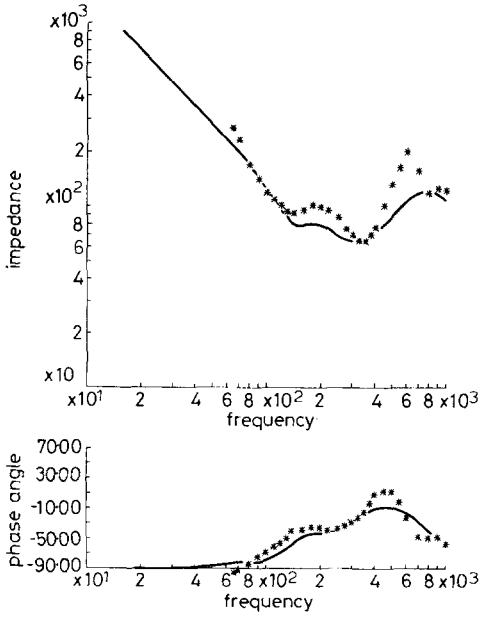

Fig. 9 Absolute impedance, $|Z|$, and phase angle, arg Z, versus forcing frequency, p
Subject CDG: 5·88 N preload.

Table 3. R.M.S. values of differences between theoretical and experimental values of absolute impedance in 80–350 Hz frequency range, N s/m

Subject	R.M.S. values N s/m
T.T. ♂	3·95
C.D.G. ♂	3·64
B.L. ♂	8·45
W.C. ♀	4·34
V.G. ♀	7·53

In general, parametric values for the remaining four subjects were generated in much the same way as for subject T.T. The shape factor, α, for computing cross-sectional moments of inertia was fixed at a value of 2·0 since ulna cross-sections are geometrically similar. Undamped resonant frequencies were initially estimated as being about 100 Hz greater than the damped resonant frequency.

The parametric values used to simulate the musculature and soft tissue were selected to give the best fit with experimental impedance data. Experiments are planned to better define the range of values for these parameters.

The correspondence between the model predictions and experimentally determined impedances for subject T.T. at a preload of 4·90 N is very good up to a forcing frequency of about 350 Hz, as shown in Fig. 5. The subresonant effect of the musculature in the 150–250 Hz region is very well simulated by the proposed model. Some loss of accuracy between model predictions occurs at lower (3·92 N) and higher (5·88 N) preloads, as shown in Figs. 4 and 6, but the overall correlation of the model with experiment is quite good up to about 350 Hz, which is close to the fundamental frequency of the excised ulna. Similarly, Fig. 8 shows the model predictions for a second subject, C.D.G., for a 4·90 N preload. Again, the correlation is quite good up to a forcing frequency of about 350 Hz. The discrepancy between the theoretical and experimental impedance at 3·92 N and 5·88 N preloads is greater for this subject than was the case for subject T.T.

Curves of the absolute impedance, $|Z|$, and phase angle, $\arg Z$, versus forcing frequency have been generated for three additional subjects, B.L., W.C. and V.G., but, for brevity, these curves are not presented here.

Instead, we compare the theoretical impedance data with the experimental data by means of the root mean square (r.m.s.) of their differences over a frequency range of 80–350 Hz.

Table 3 shows an r.m.s. for subjects T.T. and C.D.G. of 0·395 and 3·67 N s/m, respectively. The r.m.s. values for subjects B.L., W.C. and V.G. (curves not shown) are, respectively, 8·45, 4·34 and 7·53 N s/m. It should be noted that subjects W.C. and V.G. were females and the remainder were males.

In general, the correlation between the model and the experiment at forcing frequencies greater than about 350 Hz is not as good as it is below that frequency, as shown in Figs. 4–9.

Observe that in these Figures the experimental value of the absolute impedance, $|Z|$, reaches a local maximum at a frequency of about 600 Hz, whereas the theoretical curves show a local maximum at 700–800 Hz. This is unfortunate since the correlation between theory and experiment is quite good at frequencies below the first resonance, especially for subject T.T., for the parametric values used in the model.

ORNE and MANDKE (1975) speculated that the apparent 'phase' shift between the theoretical and experimental results for absolute impedance, $|Z|$, is attributable, in part, to the non-uniform distribution of stiffness and mass along the length of the ulna. Of course, detailed consideration of the variable mass and stiffness of the ulna would complicate the modelling process and, therefore, reduce its utility somewhat.

In a preliminary effort to determine the effects of ulnar nonuniformities, the ulna was analytically modelled as a tubular beam with exponential taper. It was thought that if the ratio of the second natural frequency to the fundamental frequency was significantly different from 4·0, the value for the present simply supported beam model, then it might be necessary to take into account the actual nonuniformities of the ulna if better correlation between theory and experiment at the higher frequencies is sought.

However, after applying the Rayleigh–Ritz procedure (TIMOSHENKO *et al.*, 1974) to approximate the first two natural frequencies of the beam with an exponential taper, the ratio of the first two frequencies was just a few percent greater than 4·0. The supporting derivation and calculations are not given here. Additionally, GORMAN (1975) shows similar results for a simply supported tapered beam of rectangular or elliptical cross-section. Thus, it does not appear that introduction of the nonuniform variation in the stiffness and mass along the length of the ulna into the model could account for the 'phase shift' between the theoretical predictions and experimental impedance, $|Z|$, at frequencies (350–1000 Hz) greater than the fundamental frequency of the ulna. This leads to the conclusion that the discrepancies at higher frequencies are associated more with the behaviour of the musculature and soft tissue under the impedance head than with the ulna. However, further refinements in modelling the soft tissue and musculature may not be justified since most of the useful information from the impedance tests can be obtained from data at or below the first resonance.

Conclusions

We have proposed the above *in vivo* mechanical impedance methodology in response to the need for a simple non-invasive, non-traumatic technique for *in vivo* evaluation of the status of the human skeleton. For example, in the evaluation of bone-fracture healing it would be valuable to compare the rate and degree of healing of a fractured long bone by comparing its *in vivo* mechanical impedance to the impedance of the corresponding long bone; e.g. by comparing the left ulna to the right ulna. Fracture healing can then be said to have occurred when the mechanical impedance of the fractured bone has reached, say, 95% of the mechanical impedance of the corresponding unfractured bone. In this application, only a relative comparison of the impedance of the bones in question is necessary to assess healing. However, as seen in the analysis above, the soft tissue masks the *in vivo* impedance measurements of bone; so care must be taken to compare the impedances of the bone not the impedances of the soft-hard tissue systems. Normally, some soft tissue atrophy will have occurred owing to inactivity of the fractured limb; so the soft-tissue response will be different for the two systems compared.

Additionally, in the field of biodynamics in which the response of the human body to rapid accelerations or decelerations is to be determined, it may be useful to make direct measurements of the *in vivo* mechanical properties of various parts of the body coming in contact with hard surfaces or projections within or without vehicles. For example, in the analysis of pedestrian impact situations, the force-deformation characteristics of the body at points where it contacts the striking vehicle are needed in constructing a mathematical model from which the kinematics and force response of the accident victim can be predicted. The impedance technique proposed herein can be used to obtain such force-deformation data at various loading rates *in vivo* to simulate impact conditions. Apparatus could be developed, for example, for applying a steady-state forcing function directly to the sternum in the anterior-posterior directions in order to obtain data for the chest-impact analysis problem. Similar impedance data could be obtained by measurements on cadav-

ers, but, obviously, the *in vivo* behaviour of the soft tissue would not be adequately simulated.

Finally, weightlessness in space travel, prolonged bed rest, metabolic osteoporosis or other bone dysfunctions may result in significant changes in bone strength, size and bending rigidity for which it is desirable to make direct clinical measurements. Radiographic and photon-absorption methods can provide some information on bone geometry and bone mineral content from which it is possible to estimate the structural integrity of the bone(s) in question, but direct mechanical means such as our proposed mechanical impedance technique can be used to provide a *direct* measurement of structural integrity of long bones.

However, a validated mathematical model, such as the one proposed above, is necessary for a systematic determination of Young's modulus of elasticity E, moment of inertia of bone cross-section I, and bending rigidity EI/L^3, and estimates of bone mass, all of which are related to the breaking strength of the bone.

More experiments, such as those suggested by ORNE and MANDKE (1975) are needed to give further confidence in the mathematical modelling process and to further delineate the role of the soft tissue. Once this has been done and a large statistical base of *in vivo* mechanical impedance data has been amassed, it should be possible to more clearly determine the potential of the proposed method for routine clinical and biodynamical research applications for which the methodology has been devised.

Acknowledgments—This work was supported by a NRC Postdoctoral Fellowship held by the first-named author from 1971 to 1973 at the NASA Ames Research Centre at Moffett Field, California and by NASA Grant No. -2008 with the second-named author as Principal Investigator. Both the postdoctoral fellowship and the grant were under the general supervision of the third-named author in the Life Sciences Division, NASA Ames Research Centre.

References

ANAST, G. T., FIELDS, T. and SIEGEL, I. M. (1958) Ultrasonic technique for the evaluation of bone fractures. *Am. J. Phys. Med.* **37**, 157–159.

CAMPBELL, J. N. and JURIST, J. M. (1971) Mechanical impedance of the femur: A preliminary report. *J. Biomech.* **4**, 319–322.

DOHERTY, W. P. (1971) *Dynamic response of human tibias: Application to fracture healing and osteoporosis.* Ph.D. Dissertation, Dept. of Civil Engineering, University of California, Berkeley, Cal.

GORMAN, D. J. (1975) *Free vibration analysis of beams and shafts.* J. Wiley and Sons, New York.

JURIST, J. M. (1970a) *In vivo* determination of the elastic response of bone: I. Method of ulnar resonant frequency determination. *Phys. Med. Biol.* **15**, 417–426.

JURIST, J. M. (1970b) *In vivo* determination of the elastic response of bone: II. Ulnar resonant frequency in osteoparotics, diabetics and normal subjects. *Phys. Med. Biol.* **15**, 427–434.

JURIST, J. M. and KIANIAN, K. (1973) Three models of the vibrating ulna. *J. Biomech.* **6**, 331–342.

ORNE, D. (1974) The *in vivo* driving-point impedance of the human ulna: A viscoelastic beam model. *J. Biomech.* **7**, 249–257

ORNE, D. and MANDKE, J. (1975) The influence of musculature on the mechanical impedance of the human ulna—An *in vivo* simulated study. *J. Biomech.* **8**, 143–148.

THOMPSON, G. A. (1973) *In vivo* determination of bone properties from mechanical impedance measurements. Abstracts, Aerospace Medical Association Annual Science Meeting, 7–10 May, Las Vegas, Nevada.

TIMOSHENKO, S., YOUNG, D. H. and WEAVER, W., JR. (1974) *Vibration problems in engineering*, 4th Ed., J. Wiley and Sons, New York.

Détermination '*in vivo*' des propriétés mécaniques du cubitus humain par des essais d'impédance mécanique: résultats expérimentaux et modèle mathématique amélioré

Sommaire—On décrit dans le détail une technique expérimentale et l'appareillage correspondant pour mesurer '*in vivo*' l'impédance mécanique du cubitus humain. On se sert d'un trembleur électromagnétique pour appliquer une excitation harmonique en état stationnaire au cubitus, aux environs de la mi-envergure, et on prend des mesures de l'impédance complexe du point moteur. Des informations concernant la raideur et la résonance, utiles toutes les deux pour déterminer l'intégrité mécanique de l'os, sont déduites des mesures d'impédance à l'aide d'un modèle mathématique de troisième génération (pour circuits intégrés) du système. On donne les résultats obtenus sur trois sujets masculins et deux sujets féminins.

In Vivo Bestimmung der mechanischen Eigenschaften der menschlichen Elle durch mechanische Impedanzprüfungen: Versuchsergebnisse und verbessertes mathematisches Modell

Zusammenfassung—Hierbei handelt es sich um die detaillierte Beschreibung eines Versuchsverfahrens und der hierfür eingesetzten Apparate zur Messung der mechanischen Impedanz der menschlichen Elle *in vivo*. Nahe der mittleren Ellenspanne wird zur Erzeugung einer statischen harmonischen Anregung eine elektromagnetische Schüttelvorrichtung angesetzt, und der komplexe Eingangsscheinwiderstand wird gemessen. Mit Hilfe eines mathematischen Systemmodells der dritten Generation können von den Impedanzmessungen Angaben über Steifigkeit und Resonanzfrequenz abgeleitet werden, die zur Beurteilung der mechanischen Knochenintegrität nützlich sind. Es wird über die mit drei männlichen und zwei weiblichen Versuchsobjekte erhaltenen Ergebnisse berichtet.